

Switchable polar spirals in tricolor oxide superlattices

Zijian Hong and Long-Qing Chen

Department of Materials Science and Engineering, The Pennsylvania State University, University Park, PA 16802, USA

ABSTRACT: There are increasing evidences that ferroelectric states at the nanoscale can exhibit fascinating topological structures including polar vortices and skyrmions, akin to those observed in the ferromagnetic systems. Here we report the discovery of a new type of polar topological structure, an ordered array of nanoscale spirals, in the $\text{PbTiO}_3/\text{BiFeO}_3/\text{SrTiO}_3$ tricolor ferroelectric superlattice system obtained via phase-field simulations. This polar spiral structure is composed of fine ordered semi-vortex arrays with vortex cores forming a wavy distribution. It is demonstrated that the tricolor system has an ultrahigh Curie temperature of ~ 1000 K and a temperature of ~ 800 K for the phase transformation from spiral structure to in-plane orthorhombic domain structure, demonstrating a great thermal stability. The periodicity phase-diagram is constructed, showing multiple phases from inplane domain, polar spiral, and polar vortex to flux-closure with increasing ferroelectric layer thickness. Moreover, the spiral structure has a net in-plane polarization that could be switched by an experimentally-feasible irrotational in-plane field. The switching process involves a metastable vortex state and is fully reversible. This discovery could open up a new routine to design novel multiferroic topological structures with enhanced stability and tunability towards with potential future applications in next-generation electronics.

KEYWORDS: polar spiral, thermal stability, multiferroics, switching dynamics, phase-field simulations.

Corresponding authors: Dr. Z. Hong, Email: hongzijian100@gmail.com

Z. H. now at Department of Mechanical Engineering, Carnegie Mellon University, Pittsburgh, PA, 15213.

Dr. L. -Q. Chen, Email: lqc3@psu.edu

1. Introduction

Topological structures and their phase transitions in ferroic materials have received great attention as they are not only scientifically fascinating but also have potential applications in spintronic and electronic devices such as memories and logic gates. For instance, vortices¹⁻⁶, skyrmions⁷⁻¹⁰ and merons^{11, 12} etc. were discovered in the past few decades in both ferroelectric and ferromagnetic materials. They can be manipulated by external stimuli such as magnetic/electric fields or an electric current. It is demonstrated that one can move and switch ferromagnetic vortices and skyrmions using an external electric current¹³, and their potential device applications have been proposed¹⁴. These novel topological structures with greatly reduced sizes could facilitate the miniaturization of next-generation electronic and spintronic devices. One exciting recent advance in polar topological structures and phase transitions is the discovery of the nanoscale ferroelectric vortex arrays in $(\text{PbTiO}_3)_n/(\text{SrTiO}_3)_n$ ($n=10-16$) (PTO/STO) superlattices on a DyScO_3 (DSO)

substrate^{15, 16}. While such vortex arrays are scientifically interesting, there are at least two main obstacles to realizing their device applications. Firstly, it is not trivial to switch the curl of the polar vortices by means of an irrotational electric field. Theoretical studies have demonstrated that the curl of a vortex in ferroelectrics can be switched either with a careful design of the device geometry¹⁷⁻¹⁹ or by applying an inhomogeneous or a curled electric field^{20, 21}, which however, is experimentally challenging or even unfeasible. Secondly, the polar vortex lattice is thermally unstable, favoring the formation of a_1/a_2 twin domain structures upon heating. Recent experimental and theoretical studies have shown that the vortex lattice transforms to a_1/a_2 twin domain structure gradually with increasing temperature, vanishing close to ~ 500 K²⁶.

A number of recent phase-field simulations have also shown that it is possible to control the switching of a vortex in isolated ferroelectric nanodots via thermal²², electrical²³ and mechanical stimuli^{24, 25}. However, it is challenging to fabricate and characterize those nanodots and control their electrical and mechanical boundary conditions, and thus the experimental validation of vortices in such systems has thus far been lacking.

BiFeO_3 (BFO) has long been considered as one of the most promising room temperature multiferroic materials (with both room temperature ferroelectric and G-type antiferromagnetic order), which is under extensive investigation in the past decade²⁷⁻³⁰. It has a much higher Curie temperature than other prototype ferroelectric materials (~ 1100 K³⁰, compared with PTO with Curie temperature of ~ 750 K and

BaTiO₃ with Curie temperature of 400 K). At room temperature, bulk BFO has a large spontaneous polarization ($\sim 100 \mu\text{C}/\text{cm}^2$) with a space group of $R3c$ ³⁰. So far, to the best of our knowledge, only a few vortex-like or flux-closure structures have been observed in BFO-based thin films or superlattices^{6, 31-33} since it is difficult for polarization to form continuously rotating patterns due to the strong polar anisotropy in BFO.

Here we consider a PTO/BFO/STO tricolor model system (hereafter referred as PBS-tricolor) in which the repeating unit consists of 4 unit cells of BFO sandwiched between two blocks of PTO layers (4 unit cells in each block), followed by 12 unit cells of insulating paraelectric STO layers (see the schematic of the building blocks in Figure 1). The whole film is fully strained to a (110)_o-DSO substrate (the lattice constants of substrate, PTO, BFO and STO are given in the supplementary to determine the strain conditions in each layer). In comparison, 12 unit cells of PTO and 12 unit cells of STO are periodically stacked to form a (PTO)₁₂/(STO)₁₂ superlattice (referred as PTST-superlattice with its schematic shown in Figure S1). The PBS-tricolor system can be regarded as the PTST-superlattice with the middle PTO layers substituted by BFO layers.

2. Phase-field Model

Phase-field simulations are performed by solving the time-dependent Ginzburg-Landau equations for the spatial distribution of spontaneous polarization \vec{P} :

$$\frac{\partial \vec{P}}{\partial t} = -L \frac{\delta F}{\delta \vec{P}} \quad (\text{Equation 1})$$

where t and L represent the evolution time and kinetic coefficient, respectively. F is

the total free energy of the system including contributions from elastic, electric, Landau/chemical and polarization gradient energies:

$$F = \int (f_{Elas} + f_{Elec} + f_{Land} + f_{Grad}) dV \quad (\text{Equation 2})$$

Detailed descriptions for solving the phase-field equations can be found elsewhere^{16, 34-36}. Thermodynamic potentials as well as other material constants are adopted from previous reports³⁷⁻⁴¹. The simulation system is discretized into a three dimensional mesh of 200×200×250, with each grid representing 0.4 nm. The thickness direction consists of 30 numerical grids of substrate, 192 grids of film, and 28 grids of air, respectively. Periodic boundary conditions are applied along the in-plane dimensions while the thickness direction is solved using a superposition method⁴². To obtain the electrostatic energy contribution to the polarization state, the short-circuit electric boundary condition is used by fixing the electric potential at the top and bottom of the film to 0. To perform in-plane field switching, a cyclinic homogenous in-plane electric field is applied to the film until it reaches 400 kV/cm in magnitude. To calculate the mechanical energy contribution, a thin film mechanical boundary condition is applied with a stress free condition on the film surface and zero displacements within the substrate sufficiently far away from the film/substrate interface³⁵. The iteration perturbation method is adopted to solve the elastic equilibrium equation taking into account the differences in the elastic constants among the PTO, BFO and STO layers⁴³.

3. Simulation results

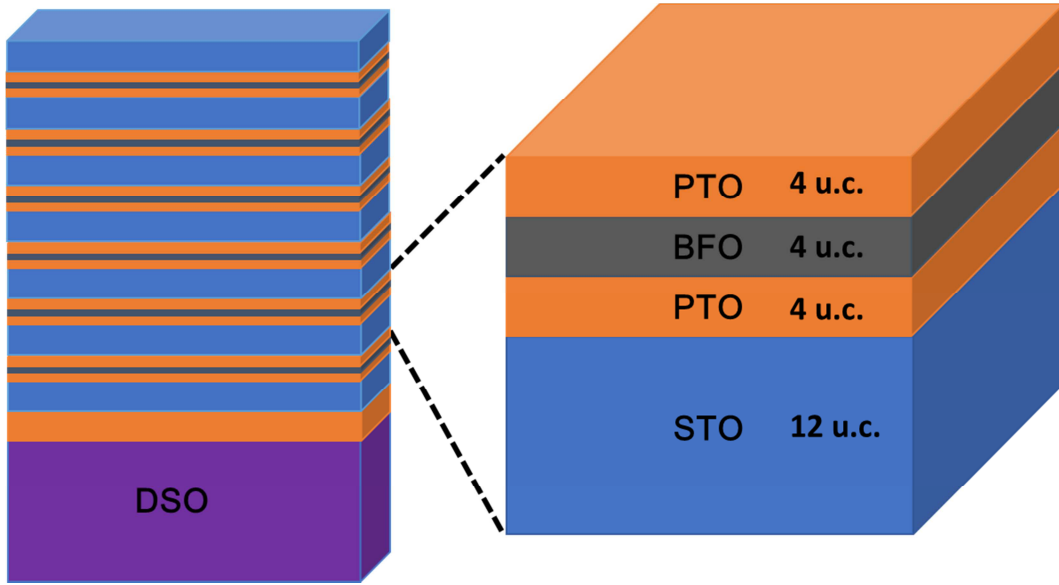


Figure 1. Schematic of the model superlattice system. Left, the whole simulation cell; right, the single periodic unit, consists of PTO, BFO, PTO, each 4 unit cells and 12 unit cells of STO.

As expected, the PTST-superlattice at room temperature exhibits an ordered array of vortices with long tube-like vortex lines, where the vortex cores are close to the center of PTO layers (Figure S2). The formation of vortex arrays within the PTST-superlattice has previously been analyzed in details^{15, 16}. Upon substitution of the middle PTO layers with BFO, one intuitive question is whether the vortex structure could be stabilized. To answer this question, the obtained polar structure of PBS-tricolor system at room temperature is plotted in Figure 2. The planar view image in Figure 2a shows that periodic long stripes form inside the PTO layers, similar to the vortex lines in the PTST-superlattice. However, these stripes are highly curved, forming a 3-dimensional wave like pattern. The zoom-in plot in Figure 2b indicates that a large P_y -component is found in the PTO layers, which causes the wave-like vortex lines. The P_y -component is largely induced by the rhombohedral BFO layer, leading to the large polarization rotation in PTO layers to account for the

symmetry mismatch between PTO and BFO layers.

The cross-section view image (Figure 2c) demonstrates that a unidirectional polar spiral structure forms, with significantly larger polarizations in the middle BFO layers. This is in contrast to the vortex lattice structure in PTST-superlattices where polarization in the cores near the middle of the PTO layers is largely reduced (see Figure S2). This can be understood since the bulk BFO has a large spontaneous polarization, and reducing the polarization in BFO layers would lead to a significant increase in the Landau/chemical energy. A magnified view in Figure 2d clearly shows that the spirals are composed of ordered arrays of alternating semi-vortices in different layers, with vortex cores floating up and down with respect to the middle BFO layers, also forming a wave-like pattern with an even smaller length scale. Due to the strong interfacial and electromechanical coupling, both the polarization in PTO and BFO layers are distorted from the corresponding bulk tetragonal and rhombohedral directions. These distortions reduce the polar discontinuity at the two interfaces, thus minimizing the surface bound charges as well as the electrostatic energy. The periodicity of the spiral is ~ 10 nm, which is close to the size of two vortices in the PTST-superlattice. Here, it is demonstrated that the substitution of middle PTO layers by BFO layers with larger polarization and a symmetry mismatch between BFO and PTO layers could lead to the formation of a unidirectional spiral structure. This can be understood since it would be energetically unfavorable for the BFO layers to adapt a nearly-tetragonal domain state to maintain a vortex structure. Instead a wavy structure forms within the rhombohedral BFO layers. Furthermore, it

costs more energy to reduce the polarization in the BFO layers than in the PTO layers, leading to the formation of vortex cores with much a smaller polarization magnitude inside the PTO layers.

In a direct comparison, the PTST-superlattice always involves the mutually counter-rotations of polarization in the neighboring vortices with minimal net polarization, giving rise to very small piezo-/dielectric- responses; whereas a spiral structure in our newly designed PBS-tricolor system has a relatively larger net in-plane polarization, which could potentially produce a larger in-plane PFM signal (Why you suddenly talked about PFM signal? Also did you ever explain what is PFM?), facilitating the characterization and ultimately the future applications of this phase.

It should be noted here that similar polar structures could also be observed in other superlattice structures with similar mismatches in lattice symmetry, lattice parameters, and ferroelectricity between the constituent layers as in the tri-color system reported here. As a matter of fact, this is a large playground for the multiferroic community to explore other novel superlattice systems, for example, by substituting part of the constituent layers with ferromagnetic/antiferromagnetic materials. This opens up possible avenues for the searching of multiferroic topological structures where the coupling between multiple order parameters can be found in nanoscale vortices/skyrmions/spirals, which is of great interest to the multiferroic community.

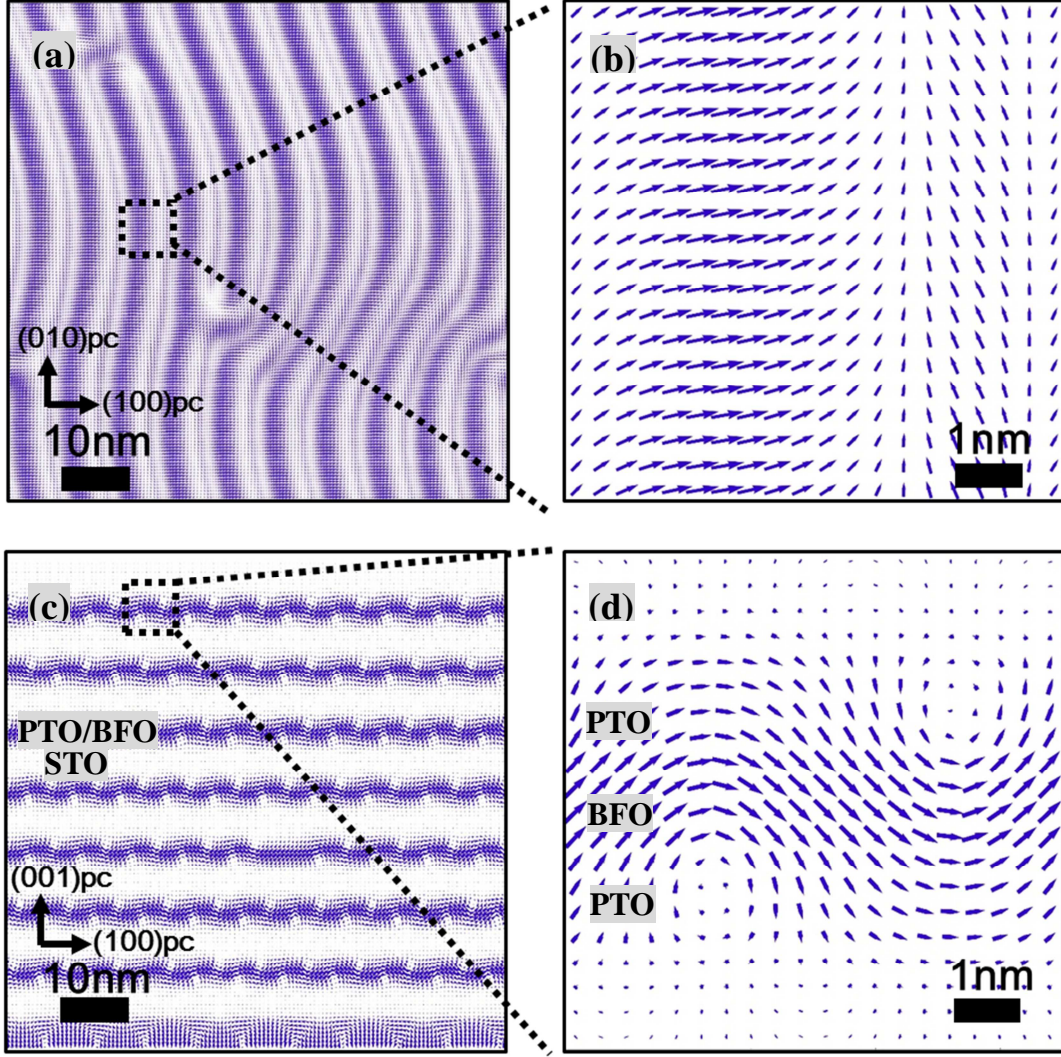


Figure 2. Polarization mapping of the tri-color system. (a) Polarization vector of the planar view in the PTO layer, showing the formation of curved stripes (b) Magnified planar view, a large y-component is clearly shown close to the main stripe. (c) Cross-section view, showing that the polar vector is forming unidirectional spirals in each layer. (d) Magnified cross-section view, showing the spirals consist of two half-vortices.

In order to reveal the thermal stability of a polar spiral phase, the temperature phase diagrams for both PBS-tricolor and PTST-superlattice systems are obtained and compared in Figure 3. The mean square of total polarization (defined as

$$\langle P^2 \rangle = \frac{\int (P_1^2 + P_2^2 + P_3^2) dV}{V})$$

is plotted with respect to temperature, which shows a

linear decay in both systems with a similar slope until reaching zero. The calculated Curie temperatures can be extracted where the linear lines intersect with zero polarization. It is discovered that the Curie temperature shows a large decrease in a PTST-superlattice as compared to bulk PTO (Curie temperature for superlattice ~650 K, for bulk PTO ~750 K), due to the large depolarization field. The decrease in Curie temperature with reducing size of ferroelectrics in ferroelectric/paraelectric superlattices as well as in ultrathin films has been well studied both theoretically^{44, 45} and experimentally^{46, 47}. For the PTST-superlattice, the Curie temperature obtained here is in good agreement with the experimentally measured value for PTO thin films grown on a (110)_o-DSO substrate under a large depolarization field⁴⁸. The Curie temperature of the PBS-tricolor system (~1000 K) is much higher than that of the corresponding PTST-superlattice system. This can be understood from two aspects: Firstly, the bulk BFO has a relatively higher Curie temperature (~1100 K) than bulk PTO (~750 K), and hence replacing PTO with BFO could increase the Curie temperature of the whole superlattice system; Secondly, a large internal field imposed by the polar BFO layers could serve as a self-poling field, which ultimately increases the Curie temperature of PTO layers. For example, a polar mapping of the high temperature phase (see Figure S3) shows that the ferroelectric BFO layers polarize the PTO layers near the BFO/PTO interfaces, where the magnitude of the induced polarization can be as high as ~0.25 C/m² at 800 K (Figure S3e).

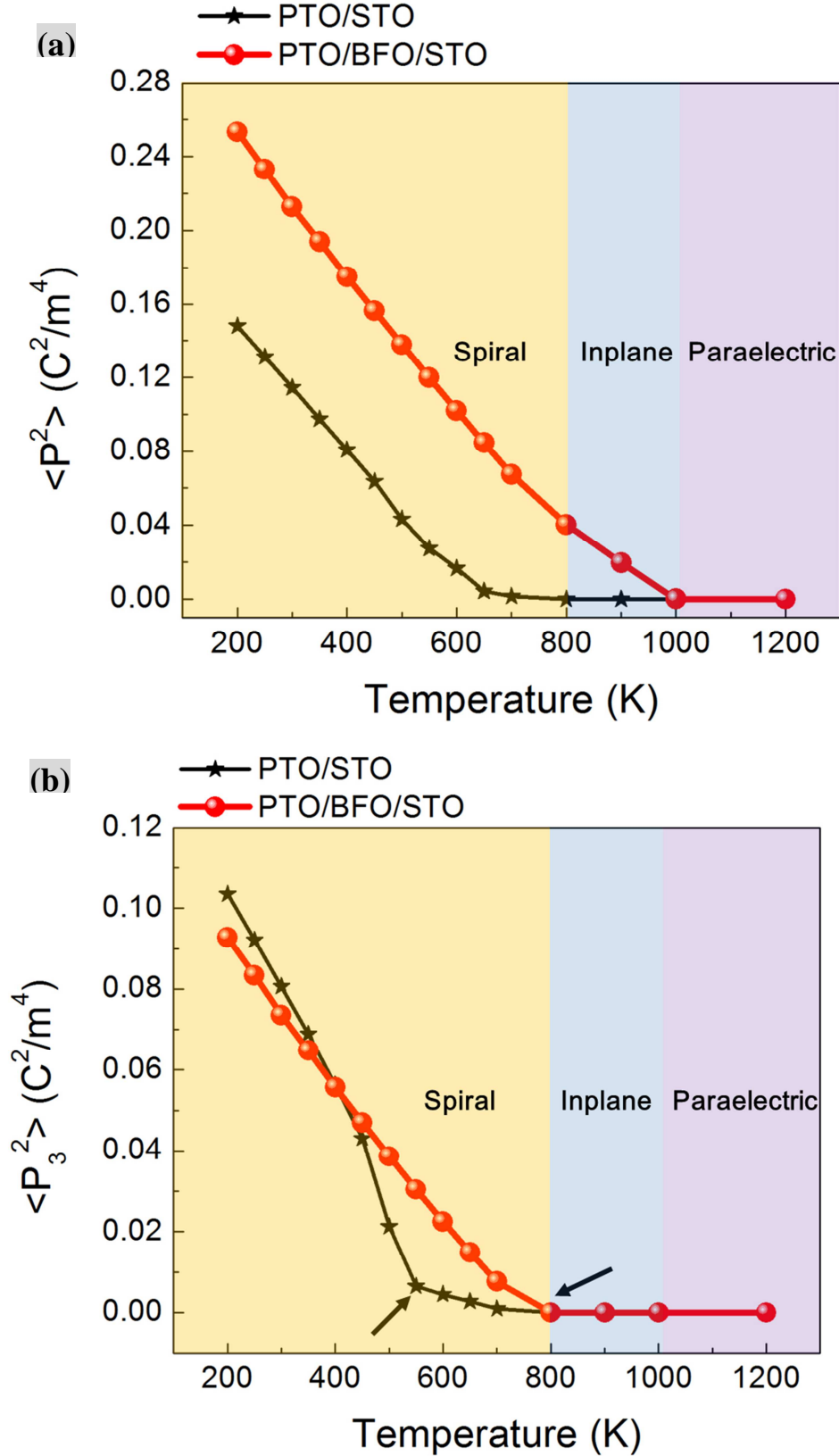


Figure 3. Temperature phase diagram of the tri-color system and a comparison with the PTST superlattice. (a) Temperature dependence of the mean square of the polarization for the tri-color system and PTST superlattice system. (b) Stability of the out-of-plane polarization,

indicating the transition between spirals (or vortex) and in-plane domains. Arrows mark the transition temperature, which shows a large increase in Curie temperature.

To get a better insight of the phase transformations for the PBS-tricolor superlattice below its Curie temperature ($\sim 1000\text{K}$), the mean square of out-of-plane polarizations

(defined as $\langle P_3^2 \rangle = \frac{\int P_3^2 dV}{V}$) is plotted as a function of temperature (see Figure 3b).

As the temperature increases, the mean square of out-of-plane polarization decreases until reaching zero at $\sim 800\text{ K}$, showing the transition from a spiral phase to complete in-plane domain structure beyond this temperature. Meanwhile, in a direct comparison, a complete transformation of vortex to a_1/a_2 in the PTST-superlattice occurs at a much lower temperature ($\sim 500\text{ K}$). One can conclude that the PBS-tricolor system exhibits a significantly increased phase transformation temperature from the topological domain to regular in-plane domain, which is unexpected. Further investigation reveals that this in-plane domain state is an orthorhombic twin structure (Figure S3). Previously, the strain-temperature phase diagram obtained by phase-field simulations indicates that orthorhombic phase can be stabilized at moderate strains with the open-circuit electric boundary condition at relatively high temperature, while experimental studies have indeed observed the orthorhombic BFO phase under a tensile substrate strain⁴⁹.

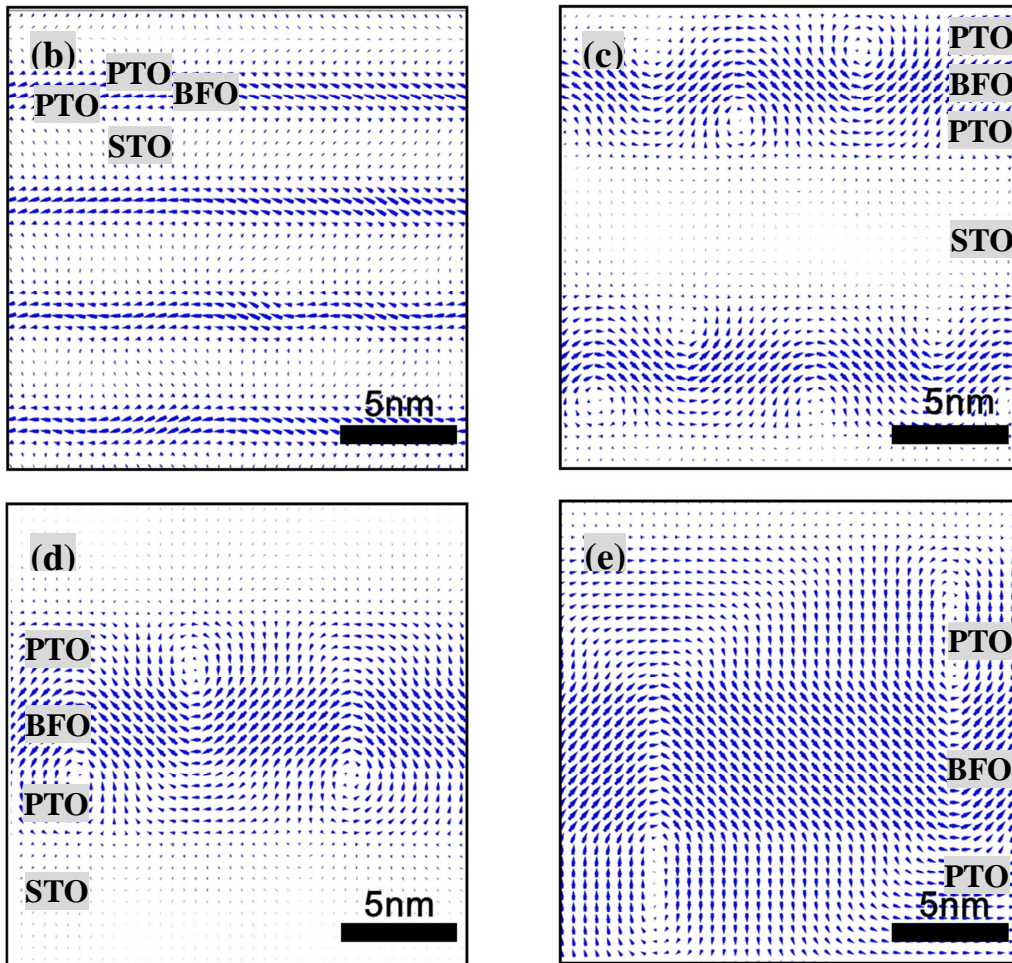
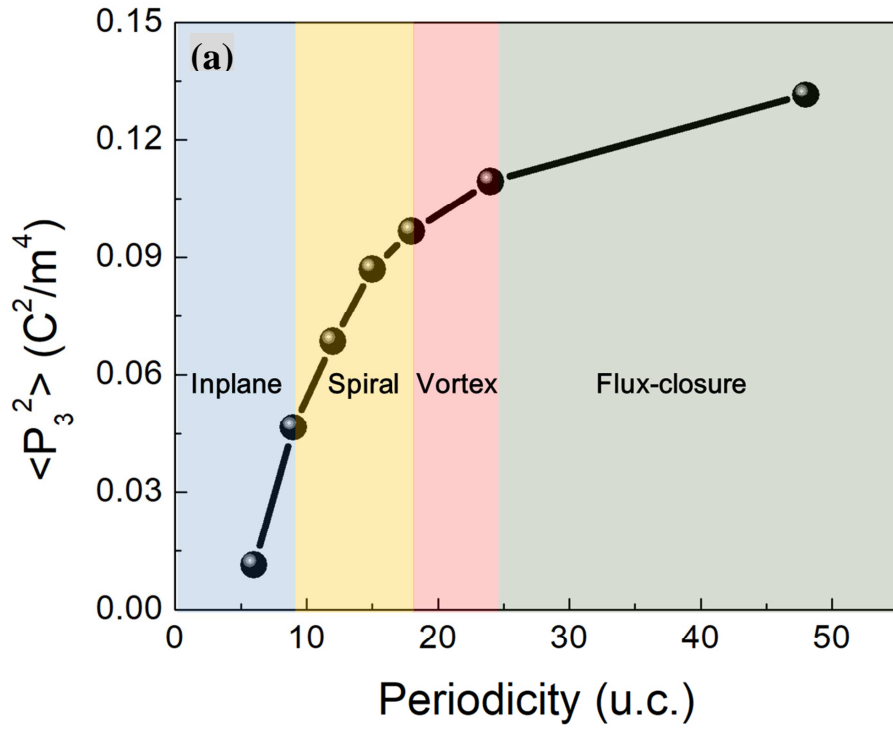


Figure 4. Periodicity phase diagram for the $(\text{PTO}_n/\text{BFO}_n/\text{PTO}_n/\text{STO}_{3n})$ tricolor superlattice on

a DyScO₃ substrate. The periodicity is defined as $3n$. (a) Mean square of the out-of-plane polarization as a function of periodicity, showing a large increase with the inplane to spiral transition and smooth increase for the spiral to vortex and vortex to flux-closure transition. (b) Inplane domain with a periodicity of 6 due to the large depolarization field. (c) Spiral phase with a periodicity of 12 and a wavy feature. (d) Vortex phase with neighboring vortices sitting on different PTO layers, forming a zigzag pattern in BFO layers, the periodicity is 24. (e) Flux-closure state at large periodicity, i.e., 48.

Previous calculations have shown that length scale of the ferroelectric layers have a great impact on the domain/polar structure for superlattice systems, due to the tunable depolarization field which decreases with increasing superlattice periodicity¹⁵.¹⁶ In Figure 4, the periodicity phase diagram is calculated for the PBS-tricolor system with a fixed ratio of individual layer thickness (i.e., PTO: BFO: STO is kept at 2:1:3). At small periodicity (i.e., $3n=6$), similar to the PTO/STO superlattice system, an inplane domain state (Figure 4b) is observed in ferroelectric layers with negligible out-of-plane polarization components. As the superlattice periodicity increases (i.e., $3n=12$), depolarization field decreases, giving rise to a huge increase in the out-of-plane polarization, forming a wavy polar feature with semi-vortex cores close to the top and bottom PTO/STO interfaces (shown in Figure 4c). A further increase in the periodicity (e.g., $3n=24$) leads to the formation of vortices in PTO layers, as depicted in Figure 4(d), whereas the vortex cores also form an up and down feature with a zig-zag pattern in BFO layers. Meanwhile, with a large superlattice periodicity of 48, (16 layers of BFO sandwiches between two 16 PTO unit cells), a flux-closure structure (Figure 4e) is formed, similar to the previous reports^{15, 16, 50}. With increasing

periodicity, the out-of-plane polarization shows a huge increase following an in-plane domain to the spiral phase transition while only a subtle increase can be found for both the spiral to vortex and vortex to flux-closure transitions, indicating that these transitions are continuous in nature.

It is worthwhile noting that this tricolor system shows a similar periodicity phase diagram as the PTO/STO superlattice and the critical length scale (~ 10 unit cells) for the formation of vortex/spiral proposed by Hong et al.¹⁵ also works here. This is due to the fact that they share the similar formula, and the decrease of depolarization field with increasing periodicity is also similar for the two systems. The spiral phase is a unique phase for the tricolor system, which forms due to the symmetry mismatch between the PTO and BFO layers, as has been shown above.

One unique feature of the spiral structure in a PBS-tricolor system as compared to the polar vortex phase in a PTST-superlattice system is that it possesses a net in-plane polarization. One natural question towards the potential applications of this novel structure would be: can we switch the net in-plane polarization direction of the spirals by an irrotational field. The electric field switching process is simulated by applying a uniform in-plane electric field (Figure 5). Initially, without an external bias, spirals are curving to the right with a net $+P_x$, consisting of periodic semi-vortices that are floating up and down. An in-plane electric field with a magnitude of 350 kV/cm is then applied, which is opposite to the initial spiral direction. This field could ultimately lead to the switching of in-plane polarization component to $-P_x$ inside the PTO layers, while the in-plane components in BFO layers are not yet switched

(Figure 5b). As a result, ordered vortex-like array structure similar to a PTST-superlattice is formed. It should be pointed out that the field-induced metastable vortex-like structure in the PBS system is not fully circular due to the difficulty in rotating the polarizations in BFO layers (in other word, BFO is more “stiff”). At even higher fields (e.g., ~ 400 kV/cm), the in-plane polarization of BFO layers switches, thus switching the direction of the spirals (Figure 5c). This structure could be stabilized even when the field is removed (Figure 5d). Further switching studies indicate that the whole process is fully reversible; with the application of a positive in-plane field, direction of spirals can be switched back to $+P_x$ again and stabilized after the applied field is removed. Here, it is shown that the directions of the spirals could be switched back and forth by experimentally accessible in-plane electric fields. Also, it should be mentioned that the reversible switching process involves multiple distinguishable states (spirals, vortex and possibly even pure a -domains), which could potentially be explored for various device applications (e.g., multiple state memory devices⁵¹, logic gates⁵², neuromorphic computing⁵³, etc.).

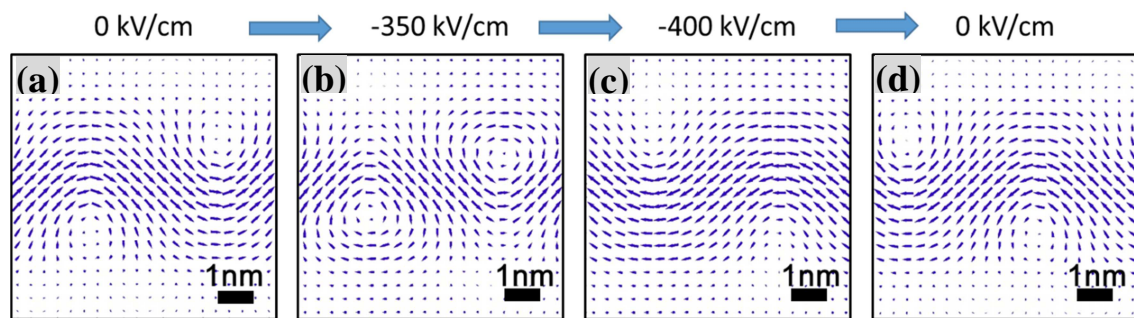


Figure 5. Switching of the spiral direction with in-plane field that is opposite to the initial spiral direction.

4. Conclusions

To conclude, we have simulated the polar structures of PTO/BFO/STO system and studied its thermal stability and switching kinetics using phase-field simulations. It is revealed that a spiral phase is formed at room temperature with semi-vortex cores floating up and down with a wave-like feature, giving rise to a net in-plane polarization. This is reminiscent of the polar vortex array structure that has been discovered in the PTST-superlattice system^{15, 16}. The PBS-tricolor system shows a greatly increased Curie temperature with enhanced thermal stability for the spiral phase as compared to the vortex lattice in the PTST-superlattice system with the substitution of some PTO layers by the high Curie temperature BFO layers. The spiral to in-plane orthorhombic domain transition temperature is even close to the Curie temperature of the PTST-superlattice (~800 K), and is much higher than the transition temperature of vortex to a_1/a_2 in the PTST-superlattice. The periodicity phase diagram is calculated for the PTST-superlattice, indicating the formation of multiple phases: including inplane domain, polar spiral, polar vortex and flux-closure as the periodicity increases. Further simulation results show that the spiral structure can be reversibly switched by experimental accessible in-plane electric fields, which involves a metastable vortex structure in-between two spiral phases with opposite in-plane directions. It has been shown that tricolor superlattices as well as $\text{BiFeO}_3/\text{PbTiO}_3$ superlattice thin films could be grown with high quality interfaces^{54-57,58}, giving promise for the experimental growth and validation of the phase-field predictions of polar structures in the proposed tricolor superlattice system. We hope that this work would stimulate more researches to discover multiferroic topological structures.

Acknowledgements:

The work is supported by the U.S. DOE, Office of Basic Energy Sciences, Division of Materials Sciences and Engineering under Award number DE-FG02-07ER46417 (ZJH and LQC) and the NSF-MRSEC grant number DMR-1420620 and NSF-MWN grant number DMR-1210588 (ZJH). ZJH would like to thank Dr. R. Ramesh for useful comments and suggestions.

References

- (1) I. Naumov, L. Bellaiche, H. Fu. Unusual phase transitions in ferroelectric nanodisks and nanorods. *Nature (London)* **432**, 737-740 (2004).
- (2) S. Choe, Y. Acremann, A. Scholl, A. Bauer, A. Doran, J. Stöhr, H. Padmore. Vortex Core-Driven Magnetization Dynamics. *Science* **304(5669)**, 420-422 (2004).
- (3) S. Bader. Colloquium: Opportunities in nanomagnetism. *Rev. Mod. Phys.* **78**, 1 (2006).
- (4) S. Prosandeev, I. Ponomareva, I. Naumov, I. Kornev, L. Bellaiche. Original Properties of Dipole Vortices in Zero-dimensional Ferroelectrics. *J. Phys.: Condens. Matter.* **20**, 193201 (2008).
- (5) T. Shinjo, T., Okuno, R. Hassdorf, K. Shigeto, T. Ono. Magnetic Vortex Core Observation in Circular Dots of Permalloy. *Science* **289 (5481)**, 930-932 (2000).
- (6) C. Nelson, B. Winchester, Y. Zhang, S. Kim, A. Melville, C. Adamo, C. Folkman, S. Baek, C. Eom, D. Schlom, L. Chen, X. Pan. Spontaneous Vortex Nanodomain Arrays at Ferroelectric Heterointerfaces. *Nano Lett.* **11 (2)**, 828–834 (2011).
- (7) N. Nagaosa, Y. Tokura. Topological Properties and Dynamics of Magnetic Skyrmions.

- Nat. Nano.* **8(12)**, 899-911 (2013).
- (8) Y. Nahas, S. Prokhorenko, L. Louis, Z. Gui, I. Kornev, L. Bellaiche. Discovery of Stable Skyrmionic State in Ferroelectric Nanocomposites. *Nat. Comm.* **6**, 8542 (2015).
- (9) J. Seidel, R. Vasudevan, N. Valanoor. Topological Structures in Multiferroics – Domain Walls, Skyrmions and Vortices. *Adv. Electron. Mater.* **2(1)**, 1500292 (2016).
- (10) Z. Hong, L. Chen. Blowing Polar Skyrmion Bubbles in Oxide Superlattices. *Acta Mater.* **152**, 155-161 (2018).
- (11) S. Wintz, C. Bunce, A. Neudert, M. Körner, T. Strache, M. Buhl, A. Erbe, S. Gemming, J. Raabe, C. Quitmann, J. Fassbender. Topology and Origin of Effective Spin Meron Pairs in Ferromagnetic Multilayer Elements. *Phys. Rev. Lett.* **110(17)**, 177201 (2013).
- (12) M. Ezawa. Compact Merons and Skyrmions in Thin Chiral Magnetic Films. *Phys. Rev. B* **83(10)**, 100408(R) (2011).
- (13) W. Jiang, P. Upadhyaya, W. Zhang, G. Yu, M. B. Jungfleisch, F. Y. Fradin, J. E. Pearson, Y. Tserkovnyak, K. L. Wang, O. Heinonen, S. G. E. te Velthuis, A. Hoffmann, Blowing magnetic skyrmion bubbles. *Science* **349**, 283 (2015).
- (14) X. Zhang, M. Ezawa, Y. Zhou. Magnetic Skyrmion Logic Gates: Conversion, Duplication and Merging of Skyrmions. *Sci. Rep.* **5**, 9400 (2015).
- (15) A. K. Yadav, C. T. Nelson, S. L. Hsu, Z. Hong, J. D. Clarkson, C. M. Schlepütz, A. R. Damodaran, P. Shafer, E. Arenholz, L. R. Dedon, D. Chen, A. Vishwanath, A. M. Minor, L. -Q. Chen, J. F. Scott, L. W. Martin, R. Ramesh, Observation of polar vortices in oxide superlattices. *Nature* **530**, 198 (2016).
- (16) Z. Hong, A. R. Damodaran, F. Xue, S. Hsu, J. Britson, A. K. Yadav, C. T. Nelson, J. Wang, J. F. Scott, L. W. Martin, R. Ramesh, L. -Q. Chen, Stability of Polar Vortex Lattice in Ferroelectric Superlattices. *Nano Lett.* **17**, 2246 (2017).

- (17) S. Prosandeev, I. Ponomareva, I. Kornev, L. Bellaiche. Control of Vortices by Homogeneous Fields in Asymmetric Ferroelectric and Ferromagnetic Rings. *Phys. Rev. Lett.* **100(4)**, 047201 (2008).
- (18) J. Wang, M. Kamlah. Intrinsic Switching of Polarization Vortex in Ferroelectric Nanotubes. *Phys. Rev. B* **80(1)**, 012101 (2009).
- (19) W. Chen, Y. Zheng, B. Wang, J. Liu. Coexistence of Toroidal and Polar Domains in Ferroelectric Systems: A Strategy for Switching Ferroelectric Vortex. *J. Appl. Phys.* **115(21)**, 214106 (2014).
- (20) S. Prosandeev, I. Ponomareva, I. Kornev, I. Naumov, L. Bellaiche. Controlling Toroidal Moment by Means of an Inhomogeneous Static Field: An Ab Initio Study. *Phys. Rev. Lett.* **96**, 237601 (2006).
- (21) J. Wang, Switching Mechanism of Polarization Vortex in Single-crystal Ferroelectric Nanodots. *Appl. Phys. Lett.* **97(19)**, 192901 (2010).
- (22) C. Wu, W. Chen, Y. Zheng, D. Ma, B. Wang, J. Liu, C. Woo. Controllability of Vortex Domain Structure in Ferroelectric Nanodot: Fruitful Domain Patterns and Transformation Paths. *Sci. Rep.* **4**, 3946 (2014).
- (23) W. Chen, Y. Zheng. Vortex Switching in Ferroelectric Nanodots and Its Feasibility by A Homogeneous Electric Field: Effects of Substrate, Dislocations and Local Clamping Force. *Acta Mater.* **88**, 41 (2015).
- (24) S. Yuan, W. Chen, L. Ma, Y. Ji, W. Xiong, J. Liu, B. Wang, Y. Zheng. Defect-mediated Vortex Multiplication and Annihilation in Ferroelectrics and The Feasibility of Vortex Switching by Stress. *Acta Mater.* **148**, 330 (2018).
- (25) Y. Zheng, W. Chen. Characteristics and Controllability of Vortices in Ferromagnetics, Ferroelectrics, and Multiferroics. *Rep. Prog. Phys.* **80 (8)**, 086501 (2017).
- (26) A. Damodaran, J. Clarkson, Z. Hong, H. Liu, A. Yadav, C. Nelson, S. Hsu, M. McCarter, K. Park, V. Kravtsov, A. Farhan, Y. Dong, Z. Cai, H. Zhou, P. Aguado-Puente, P.

- García-Fernández, J. Íñiguez, J. Junquera, A. Scholl, M. Raschke, L. -Q. Chen, D. Fong, R. Ramesh, L. Martin. Phase Coexistence and Electric-field Control of Toroidal Order in Oxide Superlattices. *Nat. Mater.* **16**, 1003-1009 (2017).
- (27) J. Wang, J. Neaton, H. Zheng, V. Nagarajan, S. Ogale, B. Liu, D. Viehland, V. Vaithyanathan, D. Schlom, V. Waghmare, N. Spaldin, K. Rabe, M. Wuttig, R. Ramesh. Epitaxial BiFeO₃ Multiferroic Thin Film Heterostructures. *Science* **299(5613)**, 1719-1722 (2003).
- (28) G. Catalan, J. Scott. Physics and Applications of Bismuth Ferrite. *Adv. Mater.* **21(24)**, 2463-2485 (2009).
- (29) R. Zeches, M. Rossell, J. Zhang, A. Hatt, Q. He, C. Yang, A. Kumar, C. Wang, A. Melville, C. Adamo, G. Sheng, Y. Chu, J. Ihlefeld, R. Erni, C. Ederer, V. Gopalan, L. Chen, D. Schlom, N. Spaldin, L. Martin, R. Ramesh. A Strain-Driven Morphotropic Phase Boundary in BiFeO₃. *Science* **326(5955)**, 977-980 (2009).
- (30) Z. Chen, J. Liu, Y. Qi, D. Chen, S. Hsu, A. Damodaran, X. He, A. N'Diaye, A. Rockett., L. Martin. 180° Ferroelectric Stripe Nanodomains in BiFeO₃ Thin Films. *Nano Lett.* **15(10)**, 6506–6513 (2015).
- (31) Y. Qi, Z. Chen, C. Huang, L. Wang, X. Han, J. Wang, P. Yang, T. Sritharan, L. Chen. Coexistence of Ferroelectric Vortex Domains and Charged Domain Walls in Epitaxial BiFeO₃ Film on (110)_O GdScO₃ Substrate. *J. Appl. Phys.* **111**, 104117 (2012).
- (32) Z. Gui, L. Wang, L. Bellaiche. Electronic Properties of Electrical Vortices in Ferroelectric Nanocomposites from Large-Scale Ab Initio Computations. *Nano Lett.* **15(5)**, 3224–3229 (2015).
- (33) F. Xue, L. Li, J. Britson, Z. Hong, C. Heikes, C. Adamo, D. Schlom, X. Pan, L. Chen. Switching the Curl of Polarization Vectors by An Irrotational Electric Field. *Phys. Rev. B* **94**, 100103(R) (2016).

- (34) L. -Q. Chen. Phase-Field Method of Phase Transitions/Domain Structures in Ferroelectric Thin Films: A Review. *J. Am. Ceram. Soc.* **91(6)**, 1835-1844 (2008).
- (35) Y. L. Li, S. Y. Hu, Z. K. Liu, L. -Q. Chen, Effect of substrate constraint on the stability and evolution of ferroelectric domain structures in thin films. *Acta Mater.* **50 (2)**, 395 (2002).
- (36) Y. L. Li, S. Y. Hu, Z. K. Liu, L. Q. Chen, Effect of electrical boundary conditions on ferroelectric domain structures in thin films. *Appl. Phys. Lett.* **81 (3)**, 427 (2002).
- (37) M. J. Haun, E. Furman, S. J. Jiang, H. A. McKinstry and L. E. Cross, Thermodynamic theory of PbTiO_3 . *J. Appl. Phys.* **62 (8)**, 3331 (1987).
- (38) G. Sheng, Y. L. Li, J. X. Zhang, S. Choudhury, Q. X. Jia, V. Gopalan, D. G. Schlom, Z. K. Liu, and L. -Q. Chen, A modified Landau-Devonshire thermodynamic potential for strontium titanate. *Appl. Phys. Lett.* **96**, 232902 (2010).
- (39) A. Tagantsev. Landau Expansion for Ferroelectrics: Which Variable to Use? *Ferroelectrics* **375**, 19-27 (2008).
- (40) Z. Chen, A. Damodaran, R. Xu, S. Lee, L. Martin. Effect of “Symmetry Mismatch” on The Domain Structure of Rhombohedral BiFeO_3 Thin Films. *Appl. Phys. Lett.* **104**, 182908 (2014).
- (41) J. Zhang, D. Schlom, L. Chen, C. Eom. Tuning the Remanent Polarization of Epitaxial Ferroelectric Thin Films with Strain. *Appl. Phys. Lett.* **95**, 122904 (2009).
- (42) L. Chen, J. Shen. Applications of Semi-implicit Fourier-spectral Method to Phase Field Equations. *Comput. Phys. Commun.* **108 (2-3)**, 147 (1998).
- (43) J. Wang, X. Ma, Q. Li, J. Britson, L. -Q. Chen, Phase transitions and domain structures of ferroelectric nanoparticles: Phase field model incorporating strong elastic and dielectric inhomogeneity. *Acta Mater.* **61(20)**, 7591 (2013).

- (44) J. Wang, T. Zhang. Size Effects in Epitaxial Ferroelectric Islands and Thin Films. *Phys. Rev. B* **73(14)**, 144107 (2006).
- (45) V. Stephanovich, I. Luk'yanchuk, M. Karkut. Domain-Enhanced Interlayer Coupling in Ferroelectric/Paraelectric Superlattices. *Phys. Rev. Lett.* **94**, 047601 (2005).
- (46) D. Fong, G. Stephenson, S. Streiffer, J. Eastman, O. Auciello, P. Fuoss, C. Thompson. Ferroelectricity in Ultrathin Perovskite Films. *Science* **304(5677)**, 1650-1653 (2004).
- (47) V. Nagarajan, S. Prasertchoung, T. Zhao, H. Zheng, J. Ouyang, R. Ramesh. Size Effects in Ultrathin Epitaxial Ferroelectric Heterostructures. *Appl. Phys. Lett.* **84(25)**, 5225-5227 (2004).
- (48) G. Catalan, A. Vlooswijk, A. Janssens, G. Rispens, S. Redfern, G. Rijnders, D. Blank, B. Noheda, X-ray Diffraction of Ferroelectric Nanodomains in PbTiO₃ Thin Films. *Integr. Ferroelectr.* **92(1)**, 18-29 (2007).
- (49) J. Yang, Q. He, S. Suresha, C. Kuo, C. Peng, R. Haislmaier, M. Motyka, G. Sheng, C. Adamo, H. Lin, Z. Hu, L. Chang, L. Tjeng, E. Arenholz, N. Podraza, M. Bernhagen, R. Uecker, D. Schlom, V. Gopalan, L. -Q. Chen, C. Chen, R. Ramesh, Y. Chu. Orthorhombic BiFeO₃. *Phys. Rev. Lett.* **109(24)**, 247606 (2012).
- (50) Y. L. Tang, Y. L. Zhu, X. L. Ma, A. Y. Borisevich, A. N. Morozovska, E. A. Eliseev, W. Y. Wang, Y. J. Wang, Y. B. Xu, Z. D. Zhang, S. J. Pennycook, Observation of a periodic array of flux-closure quadrants in strained ferroelectric PbTiO₃ films. *Science* **348**, 547 (2015).
- (51) D. Lee, S. Yang, T. Kim, B. Jeon, Y. Kim, J. Yoon, H. Lee, S. Baek, C. Eom, T. Noh. Multilevel Data Storage Memory Using Deterministic Polarization Control. *Adv. Mater.* **24(3)**, 402-406 (2012).
- (52) S. Horie, K. Noda, H. Yamada, K. Matsushige. Flexible Programmable Logic Gate using Organic Ferroelectric Multilayer. *Appl. Phys. Lett.* **91**, 193506 (2007).

- (53) D. Kuzum, S. Yu, H. Wong. Synaptic Electronics: Materials, Devices and Applications. *Nanotechnology* **24(38)**, 382001 (2013).
- (54) H. Yamada, M. Kawasaki, Y. Ogawa, Y. Tokura. Perovskite oxide tricolor superlattices with artificially broken inversion symmetry by interface effects. *Appl. Phys. Lett.* **81 (25)**, 4793-4795 (2002).
- (55) M. Kareev, Y Cao, X. Liu, S. Middey, D. Meyers, J. Chakhalian. Metallic conductance at the interface of tri-color titanate superlattices. *Appl. Phys. Lett.* **103**, 231605 (2013).
- (56) H. Lee, H. Christen, M. Chisholm, C. Rouleau, D. Lowndes. Strong polarization enhancement in asymmetric three-component ferroelectric superlattices. *Nature* **433**, 395–399 (2005).
- (57) N. Kida, H. Yamada, H. Sato, T. Arima, M. Kawasaki, H. Akoh, Y. Tokura. Optical Magnetoelectric Effect of Patterned Oxide Superlattices with Ferromagnetic Interfaces. *Phys. Rev. Lett.* **99**, 197404 (2007).
- (58) Y. Liu, Y. Zhu, Y. Tang, W. Wang, Y. Jiang, Y. Xu, B. Zhang, X. Ma. Local Enhancement of Polarization at $\text{PbTiO}_3/\text{BiFeO}_3$ Interfaces Mediated by Charge Transfer. *Nano Lett.* **17**, 3619 (2017).

Table of Contents Graphic (For Table of Contents Only)

